J Fail. Anal. and Preven. (2023) 23:361–377
https://doi.org/10.1007/s11668-022-01585-5

TECHNICAL ARTICLE—PEER-REVIEWED

Formulation of Constant Life Diagram for Fatigue Life Prediction of Glass-Carbon/Epoxy Composites

C. Hemanth Kumar · T. S. Sachit · Arunkumar Bongale

Submitted: 20 December 2022 / Accepted: 20 December 2022 / Published online: 9 January 2023

Abstract A constant life diagram (CLD) is the most common method for illustrating the relationship between stress ratios, mean stress and alternating stress. In this study, three CLD models are used to illustrate how mean stress and material anisotropy interact for several stress ratios, $R = 0.5$, 2, 0.1, -0.5, -2, and 10 to affect the fatigue life of non-hybrid $[NH]_4$ and hybrid $[H]_4$ composites. When modeling fatigue life data using each of these models, the linear piecewise model is found to be the most accurate for predicting the fatigue behavior of $[NH]_4$ and $[H]_4$ composites for all stress ratios. Using a linear piecewise model, constant life curves were able to connect all data points for each stress ratio. The *S–N* curves drawn for each stress ratio reveals that the linear model underestimates the fatigue life of non-hybrid and hybrid composites, resulting in a conservative design. Kawai's model, on the other hand, exaggerates the fatigue life of $[NH]_4$ and $[H]_4$ composites, implying an overestimation of fatigue life. As a result, designers can use a linear piecewise model to accurately predict the fatigue strength of fiber-reinforced composites for various stress ratios.

Keywords Mean stress · Constant life diagram · Stress ratio · Fatigue · Linear piecewise model · Designers

C. Hemanth Kumar (✉) · T. S. Sachit · A. Bongale
Symbiosis Institute of Technology, Pune, India
e-mail: hemanthkumar.sh17@gmail.com

C. Hemanth Kumar · T. S. Sachit · A. Bongale
Symbiosis International (Deemed University), Pune, India

Introduction

Machine parts subjected to repeated stress cycles usually fail at stress levels lower than their yield or tensile strength. This phenomenon is caused by the progressive loss of structural performance of engineering components under cyclic stressing. Information obtained from completely reversed loading conditions is insufficient for the design of machine components, which are frequently subjected to fatigue loads in addition to superimposed static loads. The two primary components of fatigue loading are mean stress and variable stress, with the former having a substantial effect on the cyclic strength of the composites [1]. Constant life diagram (CLD) depicts the influence of mean stress and anisotropy of materials on the life of machine elements subjected to fatigue loading. Due to its simplicity of construction, the conventional Goodman diagram is the constant life diagram that is most frequently used, especially for metals. However, because composite materials differ in their strengths in compression and tension, the CLD obtained from the Goodman method is insufficient to determine the fatigue strength of composites [2]. As a result, the highest point of a CLD is positioned distantly to the right from the stress ratio, $R = -1$, line for composite materials. Hence, straight lines joining alternating stress points on the 'y′ axis where the stress ratio, $R = -1$, and ultimate compressive and tensile strength points on the '*x*′ axis on the mean stress points cannot determine the influence of cyclic mean stress for composite materials. The *R* ratio, mean stress, σ_m, and alternating stress, σ_a, are the three basic factors that constitute a constant life diagram. Figure 1 depicts an example of a CLD annotation. The half-plane of the positive side of plane (σ_m–σ_a) is distributed into three regions, with the center one including

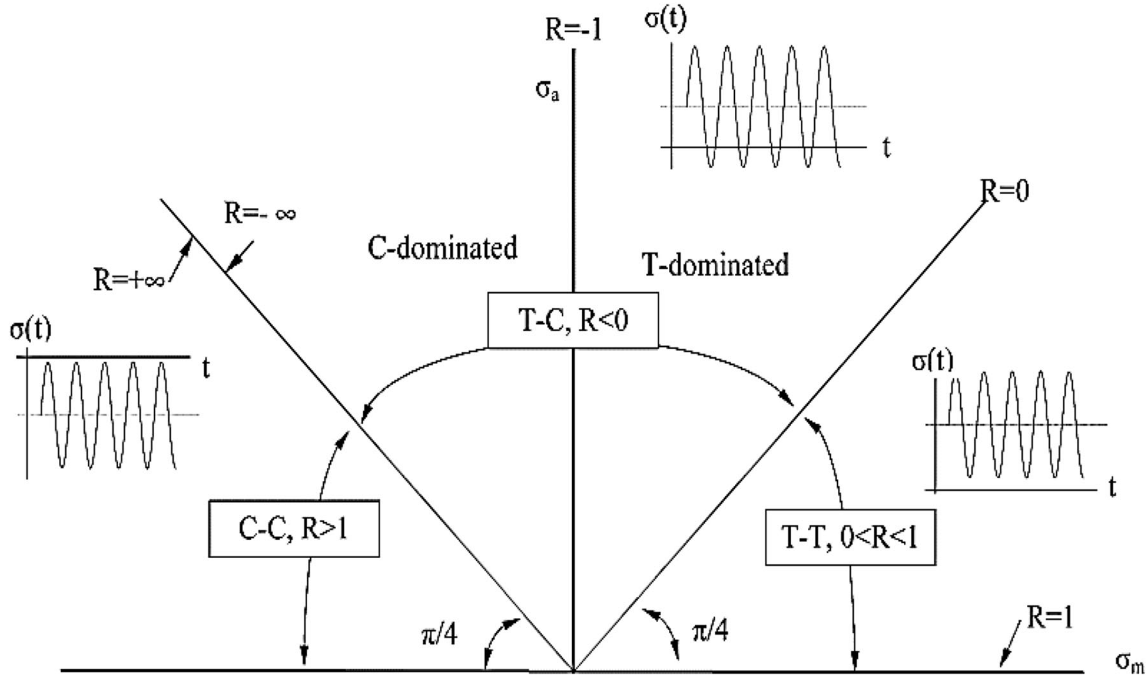

Fig. 1 A typical CLD annotation for σ_m and σ_a plane [3]

both compressive loads and mean loads. The outward lines, that represent the *S–N* diagrams at $R = 0$ and $R = 1$, signify the tension–tension (T–T) region. Positive *R* values smaller than unity are found in *S–N* curves belonging to this region. The annotations in Fig. 1 can be used to make similar observations about the other regions.

Radial lines that are emerging from the origin constitute a single SN curve and are denoted as

$$\sigma_a = \frac{(1 - R)}{(1 + R)}\sigma_m \quad \text{(Eq 1)}$$

where σ_a is alternating stress, and σ_m is mean stress, at stress ratio, *R*. The locations on the *S–N* diagram for a specific stress ratio, *R,* are indicated by the points along these radial lines. The points of consecutive radial lines, each of which corresponds to a particular number of failure cycles, are connected to form CLD. The information obtained from completely reversed loading conditions ($R = -1$) is inadequate for the design of composite materials, which are frequently subjected to fatigue loads in addition to superimposed static loads. Several alternative models for dealing with the variable characteristics of composites for varying mean stress levels have been proposed in the literature by various researchers. Nasr et al. [4] investigated the influence of mean stress on thin-walled glass fiber-reinforced composite materials under torsional stresses. The authors conducted fatigue tests at stress ratios of $R = 0, -0.25, -0.50, -0.75$, and -1. Using Goodman's equation, they found that mean stress had a negative impact on the fatigue behavior of composites. Kar et al. [5] investigated the fatigue behavior of glass-carbon fiber composite rods with varying R ratios under tension–tension loading. The fatigue behavior of composite rods was affected substantially with increase in stress levels. The influence of mean stress on the cyclic behavior of glass-polyamide composites was investigated by Mallick and Yuanxin Zhou [6]. The authors performed fatigue tests at five distinct levels of mean stress. They perceived that increasing the mean stress resulted in a substantial drop in fatigue strength of the composite specimens. This result was attributed to the creep ratcheting phenomenon during fatigue loading. Yong-Hak Huh et al. [7] conducted the axial fatigue test for three stress ratios, namely -0.2, 0.1, and 0.5. The fatigue limit of unidirectional composites was found to be lowest for a bidiagonal composite with a fiber orientation of $\pm 45°$and to be highest for a stress ratio of 0.1. For $R = -0.2$, the authors [8] discovered a similar dependence between fiber orientation and fatigue behavior. In their experimental investigation, the linear Gerber and Goodman diagram was used to calculate the fatigue life of the composites. Shaoxiong Liang et al. [9] investigated the fatigue response by applying various stress ratios to glass-flax/epoxy composites (T–T). It was found that the experimental data and Wohler's linear model had good agreement. The usefulness of CLD for predicting the fatigue life of composites was examined by Vassilopoulos et al. [10]. The authors demonstrated the use of CLD models at various stress ratios using existing experimental data sets. All these works show that it takes a significant amount of time and effort to run several experiments to obtain the required *S–N* curve for various mean stress values. To determine the fatigue response over time and with different loading scenarios, many *S–N* curves would therefore be required. Henceforth, this study employs three constant life diagram (CLD) models with only a few experimental data points to demonstrate the influence of mean stress on the fatigue strength of glass/epoxy $[NH]_4$ and glass-carbon/epoxy $[H]_4$ composites for stress ratios, $R = 0.5$, 2, 0.1, -0.5, -2, and 10.

Materials

Non-hybrid and hybrid hollow cylindrical test specimens were prepared in this study using E-glass and carbon fiber rovings, respectively, as shown in Fig. 2. Suntech Fiber Pvt., Ltd., Bengaluru, provided both fibers. Epoxy-3202 (Lapox-L-12) thermoset resin was used as a matrix material due to its excellent adhesion characteristics, fatigue strength, and high-temperature endurance. Triethylenetetramine (K-6 hardener) with a density of 950 kg/m^3 was selected to aid the curing process. Epoxy and K-6 hardener were supplied by Yuje Enterprises Bengaluru.

The volume fractions of fiber (v_G), (v_C), resin (v_R) and voids (v_v) along with the density of non-hybrid $[NH]_4$ and hybrid $[H]_4$ composites are given in Table 1.

The tensile modulus, as well as the compressive and tensile strength values of non-hybrid $[NH]_4$ and hybrid $[H]_4$ composites, are summarized in Table 2.

Constant Life Diagram (CLD) Models

The constant life curves show the distinct fatigue behavior of the materials for various combinations of amplitude and mean stress levels on the mean-amplitude plane. These areas reflect different cyclic loading regimes, as explained in Sect. "Introduction" (e.g., tension–compression). In this study, the three most widely used CLD models are used to illustrate the effect of mean stress on the fatigue life of $[NH]_4$ and $[H]_4$ composites.

a) Linear CLD [11]
b) Piecewise linear CLD [12]
c) Kawai's CLD model [13, 14]

Table 1 Volume fraction and density of composites

Composite system	Volume fraction				Density (kg/m^3)
	v_R	v_G	v_C	v_v	
Non-hybrid composites $[NH]_4$ (glass fibers/epoxy matrix)	0.4681	0.53	…	0.0019	1936.03
Hybrid composites $[H]_4$ (carbon + glass fibers/epoxy)	0.4366	0.45	0.11	0.0034	1880.01

Table 2 Tensile and compressive strength of $[NH]_4$ and $[H]_4$ composites

Composite system	Tensile modulus (MPa)	Tensile strength (UTS) in (MPa)	Compressive strength (UCS) in (MPa)
$[NH]_4$	150.52	13.25	11.73
$[H]_4$	223.50	11.78	13.18

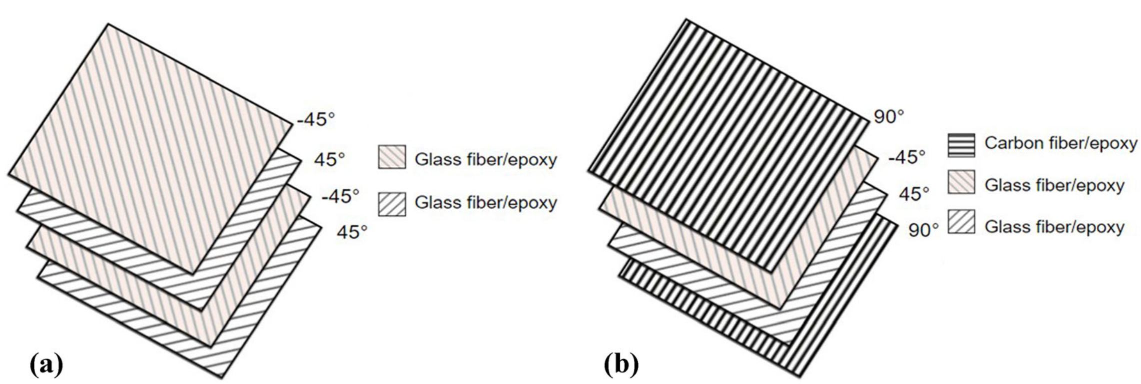

Fig. 2 Stacking arrangement of non-hybrid $[NH]_4$ and hybrid $[H]_4$ composites

Table 3 Details of applied stress levels versus number of failure cycles of $[NH]_4$ and $[H]_4$ specimens

			Number of cycles*	
Sl. No	Stress (MPa)	Load (Kg)	$[NH]_4$	$[H]_4$
1	5.30	08	260182	726034
2	6.63	10	93739	398183
3	7.95	12	33079	175169
4	9.28	14	4071	39339
5	10.60	16	390	5014
6	11.92	18	68	531

Aggregate value of 5 test specimens

Table 4 Model coefficients, k_1 and k_2 for $[NH]_4$ and $[H]_4$ composites

	$\sigma_{R=-1}$ (MPa)		k_1		k_2	
Cycles	$[NH]_4$	$[H]_4$	$[NH]_4$	$[H]_4$	$[NH]_4$	$[H]_4$
10^3	18.56	23.67	− 1.58	− 1.80	1.40	2.00
10^4	11.45	14.60	− 0.98	− 1.11	0.86	1.24
10^5	7.06	9.00	− 0.60	− 0.68	0.53	0.76
10^6	4.35	5.55	− 0.37	− 0.42	0.33	0.47
10^7	2.69	3.42	− 0.23	− 0.26	0.20	0.29

a. Linear CLD

A single *S–N* curve identified through experiment serves as the basis for the linear CLD model. This model considers fatigue test data points obtained at completely reversed loading ($R = -1$) as a basis to determine other *S–N* curves. All additional *S–N* curves can be derived from the given *S–N* curve using straightforward calculations. The constant lifeline for any *R* ratio may be determined as

$$\sigma_a = k_1\sigma_m + \sigma_{R=-1} \text{ for } \text{UCS} \le \sigma_m \le 0 \quad \text{(Eq 2)}$$

$$\sigma_a = k_2\sigma_m + \sigma_{R=-1} \text{ for } 0 \le \sigma_m \le \text{UTS} \quad \text{(Eq 3)}$$

where two factors, k_1 and k_2, are model constants and $\sigma_R = -1$ corresponds to the alternating stress amplitude fatigue data obtained at $R = -1$. UCS and UTS correspond to ultimate tensile and compressive strength values, respectively. Using Eqs 1, 2 and 3, alternating stress, σ_a, and mean stress, σ_m, can be calculated simultaneously for different stress ratios, R under consideration.

b. Piecewise Linear CLD

Linear interpolation among the data points in the (σ_m–σ_a) plane yields the desired *S–N* curve at different *R* ratios using a piecewise linear constant life diagram model. Using this model constant life diagram can also be constructed through linear interpolation between static strength data (compressive or tensile strength) and a small number of experimentally obtained fatigue data. For each portion of the CLD, the linear interpolation between uncertain and given fatigue data is done using the analytical equations. If the interpolation is done among the known *R* ratio and at

Table 5 Calculated alternating stress for $[NH]_4$ composites according to the linear model

	Alternating stress (MPa)						
Cycles /ratio	2	10	− 2	− 1	0.1	− 0.5	0.5
10^3	3.23	6.30	12.14	18.56	6.89	12.65	3.44
10^4	2.92	5.20	8.63	11.45	5.55	8.86	3.18
10^5	2.52	4.05	5.87	7.06	4.26	6.00	2.72
10^6	2.06	3.00	3.87	4.35	3.10	3.92	2.19
10^7	1.60	2.10	2.50	2.69	2.16	2.52	1.67

Table 6 Calculated mean stress for $[NH]_4$ composites according to the linear model

	Mean stress (MPa)						
Cycles/ratio	2	10	− 2	− 1	0.1	− 0.5	0.5
10^3	9.69	7.75	4.06	0	8.48	4.23	10.31
10^4	8.75	6.40	2.89	0	6.83	2.97	9.57
10^5	7.55	4.98	1.96	0	5.25	2.00	8.14
10^6	6.18	3.68	1.30	0	3.81	1.31	6.58
10^7	4.78	2.58	0.84	0	2.65	0.84	5.01

Table 7 Calculated alternating stress for $[H]_4$ composites according to the linear model

	Alternating stress (MPa)						
Cycles/ratio	2	10	− 2	− 1	0.1	− 0.5	0.5
10^3	3.70	7.38	14.80	23.67	6.84	14.19	3.38
10^4	3.37	6.18	10.66	14.60	5.81	10.32	3.09
10^5	2.95	4.89	7.33	9.00	4.64	7.17	2.74
10^6	2.46	3.66	4.86	5.55	3.52	4.80	2.30
10^7	1.93	2.60	2.47	3.42	2.52	3.12	1.83

Table 8 Calculated mean stress for $[H]_4$ composites according to the linear model

	Mean stress (MPa)						
Cycles/ratio	2	10	− 2	− 1	0.1	− 0.5	0.5
10^3	11.12	9.08	4.94	0	8.42	4.74	10.14
10^4	10.13	7.60	3.56	0	7.15	3.45	9.28
10^5	8.86	6.01	2.45	0	5.71	2.40	8.20
10^6	7.36	4.50	1.63	0	4.32	1.60	6.90
10^7	5.78	3.19	0.83	0	3.10	1.04	5.49

Table 9 Calculated alternating stress for $[NH]_4$ composites according to piecewise linear model

Cycles/ratio	Alternating stress (MPa)						
	2	10	− 2	− 1	0.1	− 0.5	0.5
10^3	3.23	6.3	12.14	18.56	6.84	12.65	3.57
10^4	2.92	5.20	8.64	11.45	5.57	8.89	3.19
10^5	2.52	4.06	5.88	7.06	4.28	6.00	2.72
10^6	2.05	2.99	3.87	4.35	3.11	3.92	2.20
10^7	1.60	2.10	2.50	2.69	2.15	2.52	1.67

Table 10 Calculated mean stress for $[NH]_4$ composites according to piecewise linear model

Cycles/ratio	Mean stress (MPa)						
	2	10	− 2	− 1	0.1	− 0.5	0.5
10^3	9.69	7.75	4.05	0	8.41	4.23	10.71
10^4	8.76	6.40	2.89	0	6.85	2.97	9.57
10^5	7.56	4.99	1.96	0	5.26	2.00	8.16
10^6	6.15	3.68	1.29	0	3.83	1.31	6.60
10^7	4.80	2.58	0.84	0	2.64	0.84	5.01

Table 11 Calculated alternating stress for $[H]_4$ composites according to piecewise linear model

Cycles/ratio	Alternating stress (MPa)						
	2	10	− 2	− 1	0.1	− 0.5	0.5
10^3	3.71	7.39	14.80	23.67	6.82	14.16	3.37
10^4	3.38	6.19	10.66	14.60	5.79	10.32	3.10
10^5	2.96	4.90	7.33	9.00	4.64	7.71	2.74
10^6	2.46	3.66	4.87	5.55	3.52	4.80	2.30
10^7	1.93	2.60	3.15	3.42	2.52	3.12	1.82

Table 12 Calculated mean stress for $[H]_4$ composites according to piecewise linear model

	Mean stress (MPa)						
Cycles/ratio	2	10	− 2	− 1	0.1	− 0.5	0.5
10^3	11.13	9.09	4.94	0	8.39	4.73	10.11
10^4	10.14	7.61	3.56	0	7.12	3.45	9.30
10^5	8.88	6.03	2.45	0	5.71	2.58	8.22
10^6	7.38	4.50	1.63	0	4.33	1.60	6.90
10^7	5.79	3.20	1.05	0	3.10	1.04	5.46

$R = 1$, in the tension–tension section, then unknown alternating stress, $\sigma_{a'}$, is determined by Eq 4.

$$\sigma_{a\prime} = \frac{\mathrm{UTS}}{\left(\frac{\mathrm{UTS}}{\sigma_{a'1\mathrm{TT}}}\right) + r' - r_{1\mathrm{TT}}} \quad \text{(Eq 4)}$$

Table 13 Parameters calculated for $[NH]_4$ composites according to Kawai's model

Cycle	$\sigma_{max}{}^{\gamma}$(MPa)	φ_γ	σ_B(MPa)
10^3	18.56	1.40	13.25 (UTS)
10^4	11.45	0.87	
10^5	7.06	0.53	
10^6	4.35	0.33	
10^7	2.69	0.20	

where UTS = tensile strength, $\sigma_{a'1TT}$ = stress amplitude obtained from the fatigue test, r' is the unknown stress ratio, and r_{1TT} is the known stress ratio. If the interpolation is done between $R = 1$ and known R ratio, in the compression–compression region, then unknown alternating stress, $\sigma_{a'}$, is determined by

$$\sigma_{a\prime} = \frac{\mathrm{UTC}}{\left(\frac{\mathrm{UTC}}{\sigma_{a'1\mathrm{CC}}}\right) + r' - r_{1\mathrm{CC}}} \quad \text{(Eq 5)}$$

where UTC = compressive strength, $\sigma_{a'1CC}$ = stress amplitude obtained from the fatigue test, r' is the unknown stress ratio, and r_{1CC} is the known stress ratio. The following equation can be used for linear interpolation if R lies between two R ratios ($R_i + R_{i+1}$).

$$\sigma'_a = \frac{\sigma_{a,i}(r_i - r_{i+1})}{(r_i - r')\left(\frac{\sigma_{a,i}}{\sigma_{a,i+1}}\right) + (r\prime - r_{i+1})} \quad \text{(Eq 6)}$$

where $\sigma_{a,\ i}$ is the known (first) alternating stress at $R = R_i$ and r_i is the known (first) stress ratio.

c. Kawai's CLD

The fundamental tenet of the Kawai CLD model is that as fatigue life increases, the form of the constant failure curves shifts to a parabola from straight line. The static failure envelope according to Kawai is indicated as two straight lines joining compressive and tensile strength, which is bounded by the CLD with maximum alternating stress on the experimentally determined *S–N* curve. This model allows the designers to construct an *S–N* curve at desired *R* ratio by varying different mean and alternating stress components with the help of a single experimentally acquired *S–N* curve. Thus, the resulting anisomorphic constant life diagram, developed by Kawai and Koizumi, is asymmetric and is described by Eqs 7 and 8.

$$\frac{\sigma_a^\gamma - \sigma_a}{\sigma_a^\gamma} = \left(\frac{\sigma_m - \sigma_m^\gamma}{\mathrm{UTS} - \sigma_m^\gamma}\right)^{2-\varphi_\gamma} \text{for UTS} \geq \sigma_m \geq \sigma_m^\gamma \quad \text{(Eq 7)}$$

$$\frac{\sigma_a^\gamma - \sigma_a}{\sigma_a^\gamma} = \left(\frac{\sigma_m - \sigma_m^\gamma}{\mathrm{UCS} - \sigma_m^\gamma}\right)^{2-\varphi_\gamma} \text{for UCS} \geq \sigma_m \geq \sigma_m^\gamma \quad \text{(Eq 8)}$$

Table 14 Calculated alternating stress for $[NH]_4$ composites according to Kawai's model

Cycles/ratio	Alternating stress (MPa)						
	2	10	− 2	− 1	0.1	− 0.5	0.5
10^3	2.94	5.38	9.89	18.56	5.78	10.30	3.22
10^4	3.00	5.42	9.00	11.45	5.79	9.26	3.28
10^5	2.78	4.62	6.47	7.06	4.86	6.55	3.02
10^6	2.41	3.53	4.23	4.35	3.65	4.26	2.58
10^7	1.93	2.46	2.66	2.69	2.50	2.67	2.03

Table 15 Calculated mean stress for $[NH]_4$ composites according to Kawai's model

Cycles/ratio	Mean stress (MPa)						
	2	10	− 2	− 1	0.1	− 0.5	0.5
10^3	8.82	6.61	3.30	0	7.11	3.44	9.66
10^4	9.00	6.67	3.00	0	7.13	3.10	9.84
10^5	8.34	5.68	2.16	0	5.98	2.19	9.06
10^6	7.23	4.34	1.42	0	4.49	1.43	7.74
10^7	5.79	3.02	0.89	0	3.08	0.89	6.09

Table 16 Parameters calculated for $[H]_4$ composites according to Kawai's model

Cycle	$\sigma_{max}{}^{\gamma}$(MPa)	φ_{γ}	σ_B(MPa)
10^3	23.67	1.80	13.20 (UCS)
10^4	14.60	1.10	
10^5	9.00	0.68	
10^6	5.55	0.42	
10^7	3.42	0.26	

Table 17 Calculated alternating stress for $[H]_4$ composites according to Kawai's model

Cycles /ratio	Alternating stress (MPa)						
	2	10	− 2	− 1	0.1	− 0.5	0.5
10^3	2.51	4.12	6.95	23.67	3.90	6.70	2.34
10^4	3.30	5.97	10.10	14.60	5.59	9.89	3.02
10^5	3.16	5.38	7.92	9.00	5.09	7.78	2.92
10^6	2.81	4.26	5.31	5.55	4.09	5.27	2.62
10^7	2.30	3.04	3.37	3.42	2.98	3.36	2.19

where σ_a^{γ} and σ_m^{γ} are alternating and mean stress components that are experimentally obtained from fatigue stress values at critical stress ratio, $R = -1$ and

Table 18 Calculated mean stress for $[H]_4$ composites according to Kawai's model

	Mean stress (MPa)						
Cycles/ratio	2	10	− 2	− 1	0.1	− 0.5	0.5
10^3	7.53	5.06	2.32	0	4.80	2.24	7.02
10^4	9.90	7.34	3.37	0	6.88	3.31	9.06
10^5	9.48	6.62	2.64	0	6.26	2.60	8.76
10^6	8.43	5.24	1.77	0	5.03	1.76	7.86
10^7	6.90	3.74	1.12	0	3.67	1.12	6.57

$$\varphi_{\gamma} = \frac{\sigma_{\max}^{\gamma}}{\sigma_B} \quad \text{(Eq 9)}$$

φ_{γ} represents the ratio of the stress,$\sigma_{\max}^{\gamma}$ is obtained from the experimental data for the critical SN curve to the maximum stress,σ_B (absolute) value between tensile strength and compressive strength.

These three models can be used to estimate the amplitude and mean stresses under different loading situations for which there is no experimental data. In this work, fatigue cycles count was varied from 10^3 to 10^7 to get a clear understanding of stress ratios and to handle a wide variety of loading options between maximum compressive strength (UCS) and maximum tensile strength (UTS), the models were fitted using the corresponding equations, across the entire range of mean stress values.

Results and Discussion

Using an in-house built rotational bending fatigue machine as described in reference [15], fatigue tests were performed at a stress ratio of $R = -1$ at an operating frequency of 10 Hz, to investigate the fatigue strength of composite specimens for different stress ratios using CLD models. Six stress levels were chosen as a reference for constant amplitude fatigue testing at room temperature, covering "high stress-low cycle" and "low stress-high cycle" fatigue regimes, as illustrated in Table 3 with the number of failure cycles.

Fatigue Life Modeling

a. Linear CLD

Two model coefficients, k_1 and k_2, are determined by solving Eqs 2 and 3 at the UTS and UCS points of $[NH]_4$ and $[H]_4$ composite specimens.

$$k_{1=-}\frac{\sigma_{R=-1}}{\text{UCS}} \quad \text{(Eq 10)}$$

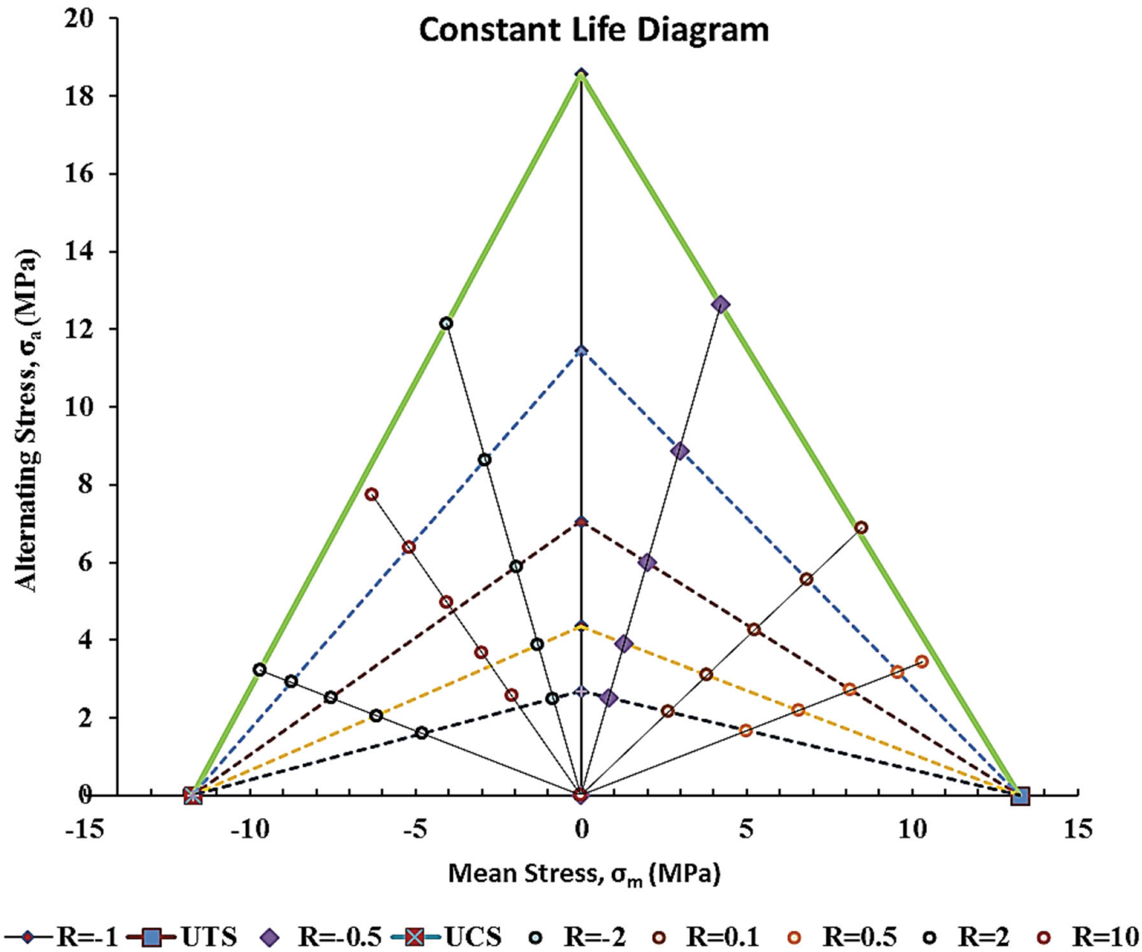

Fig. 3 CLD for $[NH]_4$ specimens according to the linear model

$$k_{2=-}\frac{\sigma_{R=-1}}{\mathrm{UTS}} \quad \text{(Eq 11)}$$

The corresponding results of model coefficients, k_1 and k_2, for several cycles ranging from 10^3 to 10^7 under "low stress-high cycle" fatigue are depicted in Table 4.

The calculated alternating and mean stress for $[NH]_4$ composites using the linear model is depicted in Tables 5 and 6, respectively.

Similarly, the calculated alternating and mean stress for $[H]_4$ composites is depicted in Tables 7 and 8, respectively.

b. Piecewise Linear CLD

For different regions of the CLD, the alternating and mean stress are computed using the Eqs. 4, 5, and 6. The calculated alternating and mean stress for $[NH]_4$ composites using a piecewise linear model are depicted in Tables 9 and 10 respectively.

Similarly, the calculated alternating and mean stress for $[H]_4$ composites is depicted in Tables 11 and 12, respectively.

c. Kawai's CLD Model

For Kawai's CLD model, fatigue loading data with $R = -1$ were applied. This stress ratio is commonly referred to as the critical stress ratio. For different regions of the CLD, the alternating and mean stress are computed using Eq 7 and 8. For different sections of the CLD, constant life curves were constructed using a sixth-order polynomial function. Tables 13 and 16 show the

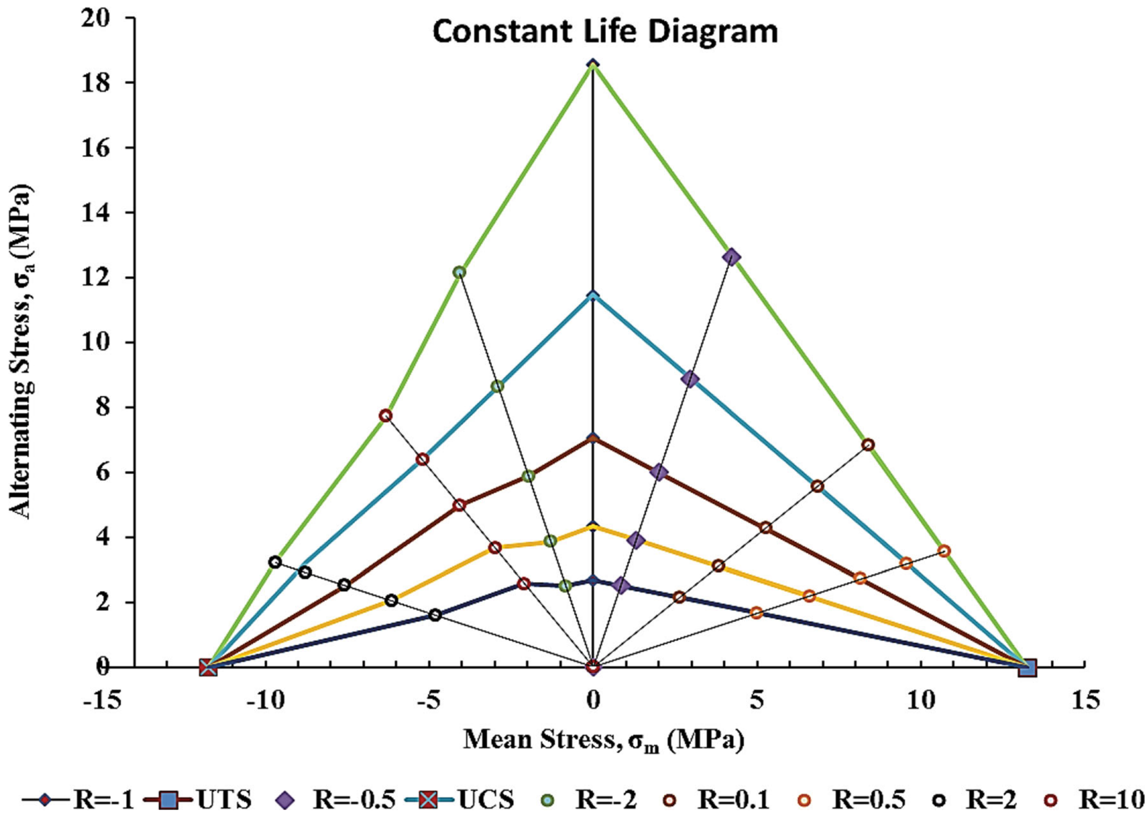

Fig. 4 CLD for $[NH]_4$ specimens according to piecewise linear model

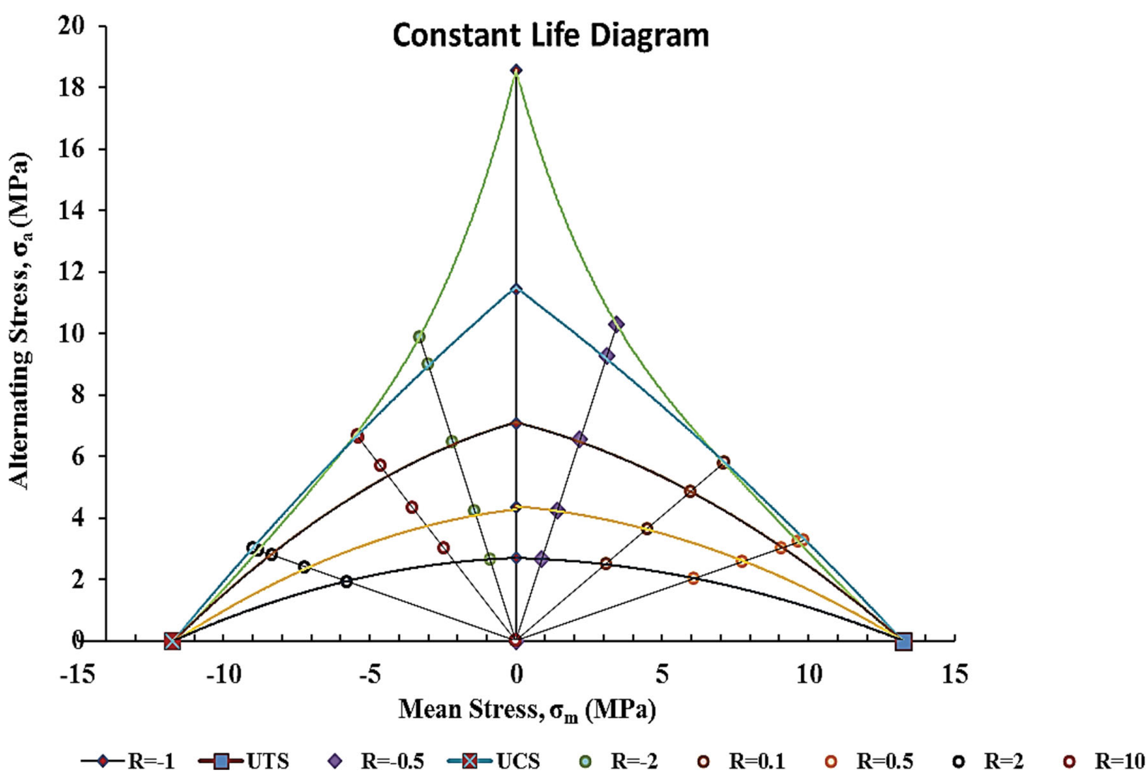

Fig. 5 CLD for $[NH]_4$ specimens according to Kawai's model

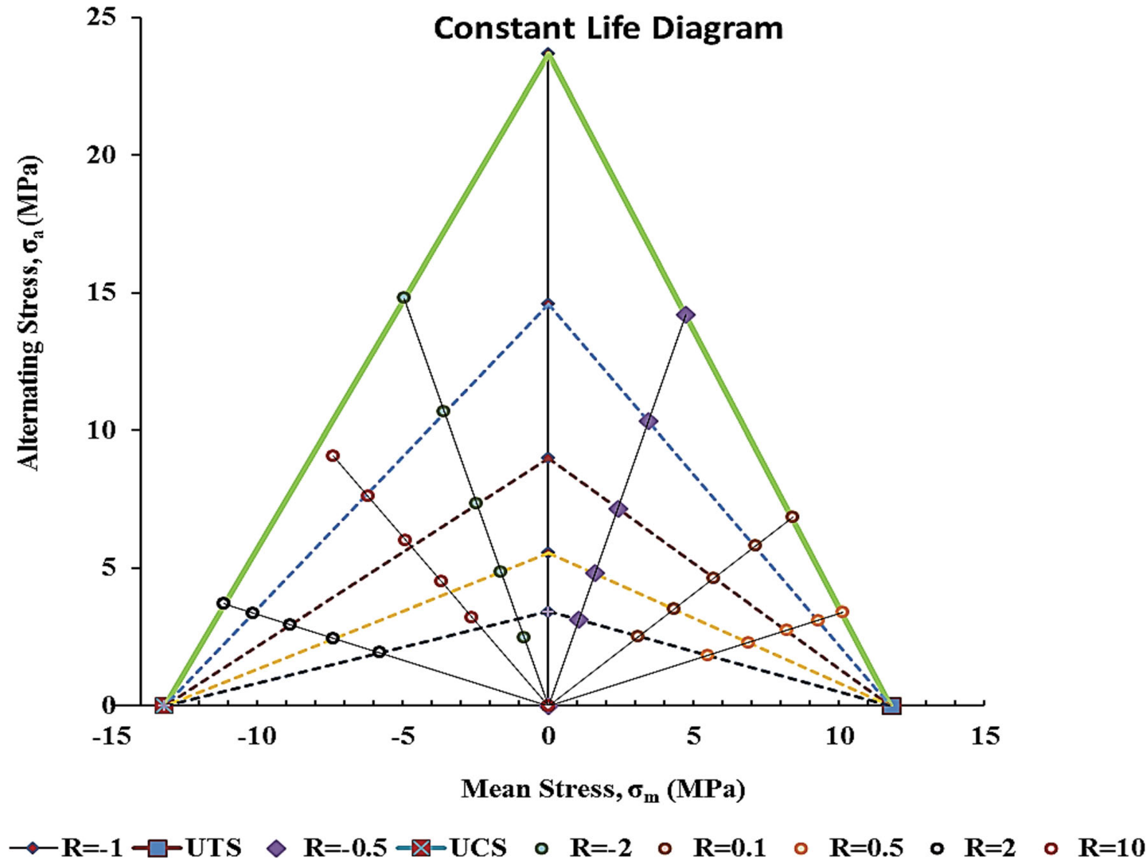

Fig. 6 CLD for $[H]_4$ specimens according to the linear model

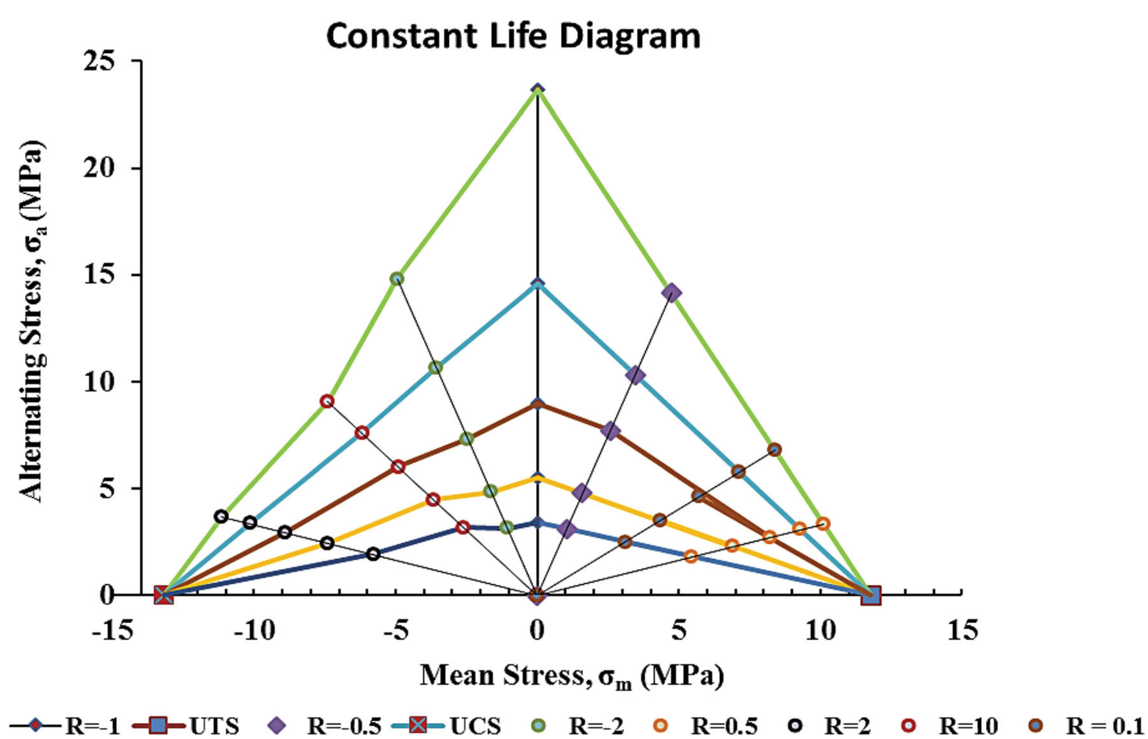

Fig. 7 CLD for $[H]_4$ specimens according to piecewise linear model

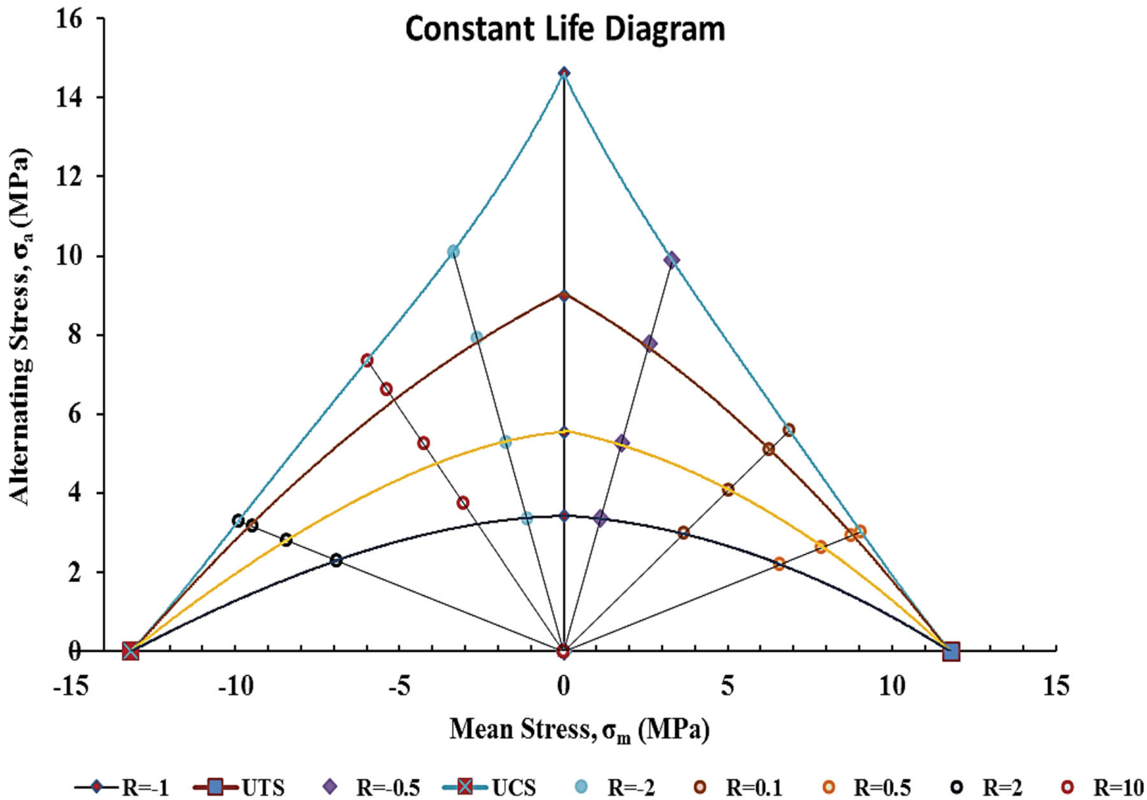

Fig. 8 CLD for $[H]_4$ specimens according to Kawai's model

Table 19 Comparison of the coefficient of correlation (R^2) for predictive power function for $[NH]_4$ composites

	R ratio for $[NH]_4$ composites					
	0.5	2	0.1	− 0.5	− 2	10
Linear CLD model	0.96	0.97	0.98	0.99	0.98	0.98
Piecewise linear CLD model	0.97	0.97	0.99	0.99	0.99	0.99
Kawai's CLD model	0.95	0.95	0.97	0.96	0.98	0.93

Table 20 Comparison of the coefficient of correlation (R^2) for predictive power function $[H]_4$ composites

	R ratio for $[H]_4$ composites					
	0.5	2	0.1	− 0.5	− 2	10
Linear CLD model	0.94	0.96	0.97	0.99	0.97	0.98
Piecewise linear CLD model	0.98	0.98	0.98	0.99	0.99	0.99
Kawai's CLD model	0.91	0.92	0.95	0.96	0.97	0.94

parameters computed for this model, as stated in Eq 9 for $[NH]_4$ and $[H]_4$ specimens, respectively.

The calculated alternating and mean stress components for $[NH]_4$ composites using Kawai's model are depicted in Tables 14 and 15, respectively.

The calculated alternating and mean stress components for $[H]_4$ composites using Kawai's model are depicted in Tables 17 and 18, respectively.

Constant Life Diagram (CLD)

When modeling fatigue life of $[NH]_4$ and $[H]_4$ composite specimens for different stress ratios (*R*), the linear model has a lower level of accuracy when the stress ratio is 0.5 and 10 as shown in Fig. 3 for $[NH]_4$ composites. The mean stress component increases from ultimate compressive strength to zero, with alternating stress having a greater value in compression-predominant areas. With decreasing alternating stress in the tension-dominating zone, mean stress increases from zero to ultimate tensile strength. Figure 6 demonstrates that when the stress ratio is 10, the linear model for $[H]_4$ composites becomes less reliable. Constant life curves for $[NH]_4$ and $[H]_4$ composites were able to connect accurately with all the points for the

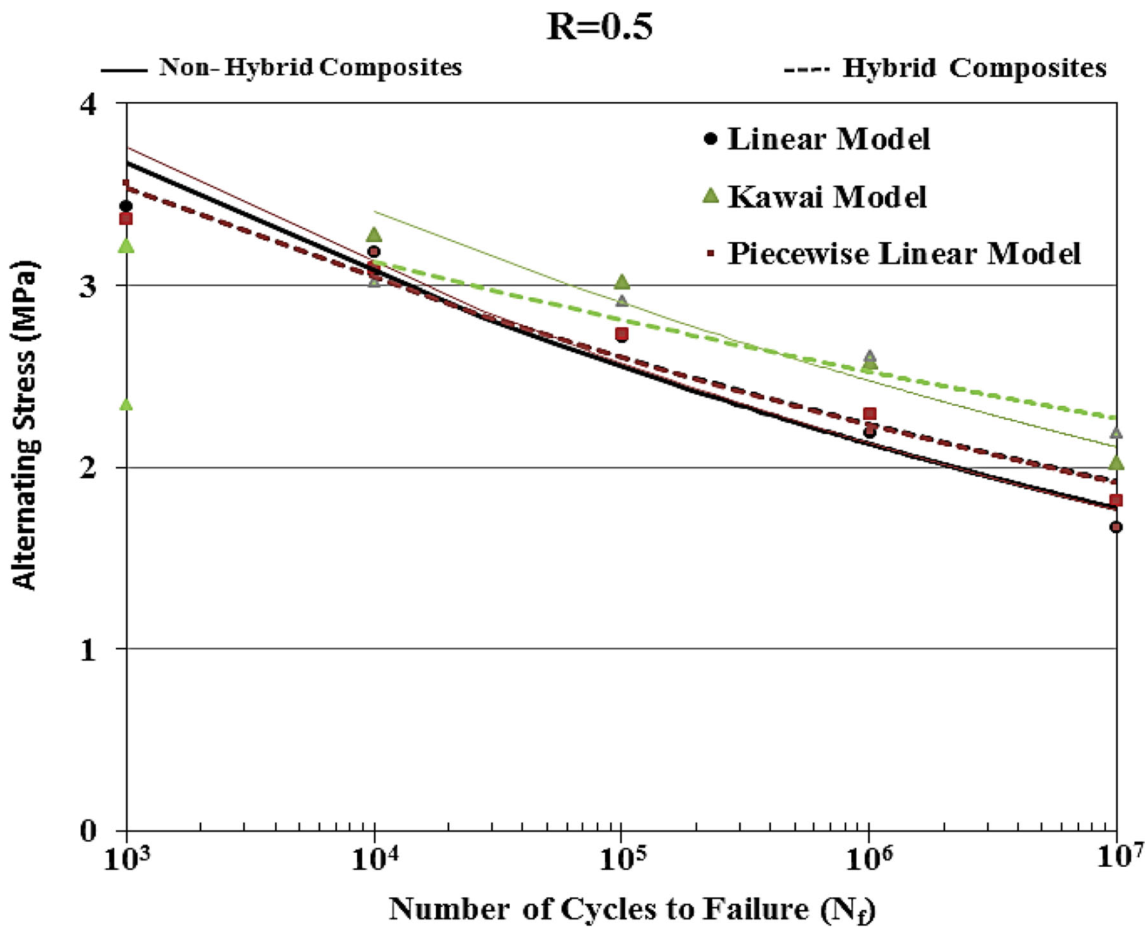

Fig. 9 *S–N* curves for $[NH]_4$ and $[H]_4$ composites at R = 0.5

specified stress ratios using the linear piecewise CLD, as shown in Figs. 4 and 7. Kawai's model, on the other hand, is less accurate when R = 10 for $[NH]_4$ and $[H]_4$ composites, as shown in Figs. 5 and 8. This model's main shortcoming is that it cannot predict the effect of mean stress at larger stress amplitudes for shorter life cycles. The constant life curves follow a second-order polynomial function as the cycles to failure increase, as shown in Figs. 5 and 8. As a result, designers can precisely construct continuous life diagrams for fiber-reinforced composites using piecewise linear CLD model.

Comparison of CLD Models

When modeling fatigue data with stress ratios R = 0.5, 2, 0.1, – 0.5, – 2, and 10 using each of these models, the linear piecewise model is extremely accurate for predicting the fatigue behavior of $[NH]_4$ and $[H]_4$ composites for all stress ratios. By joining all the data points for the specified stress ratios, R, constant life curves were successfully formulated using linear piecewise model. The assumption that the fatigue life data must be fitted with a power law function forms the basis for all the derived constant life diagrams. The predictive power of each of the employed models was evaluated. The R^2 value of predicted curves for $[NH]_4$ and $[H]_4$ composites values is shown in Tables 19 and 20.

Figures 9, 10, 11, 12, 13, and 14 show the *S–N* diagrams that were constructed for each stress ratio (R) using each of these models. Since it is not derived on any assumptions, the piecewise linear model is inherently more stable than other two models. The linear model understates the fatigue life of the $[NH]_4$ and $[H]_4$ composites for all stress ratios investigated, resulting in a conservative design

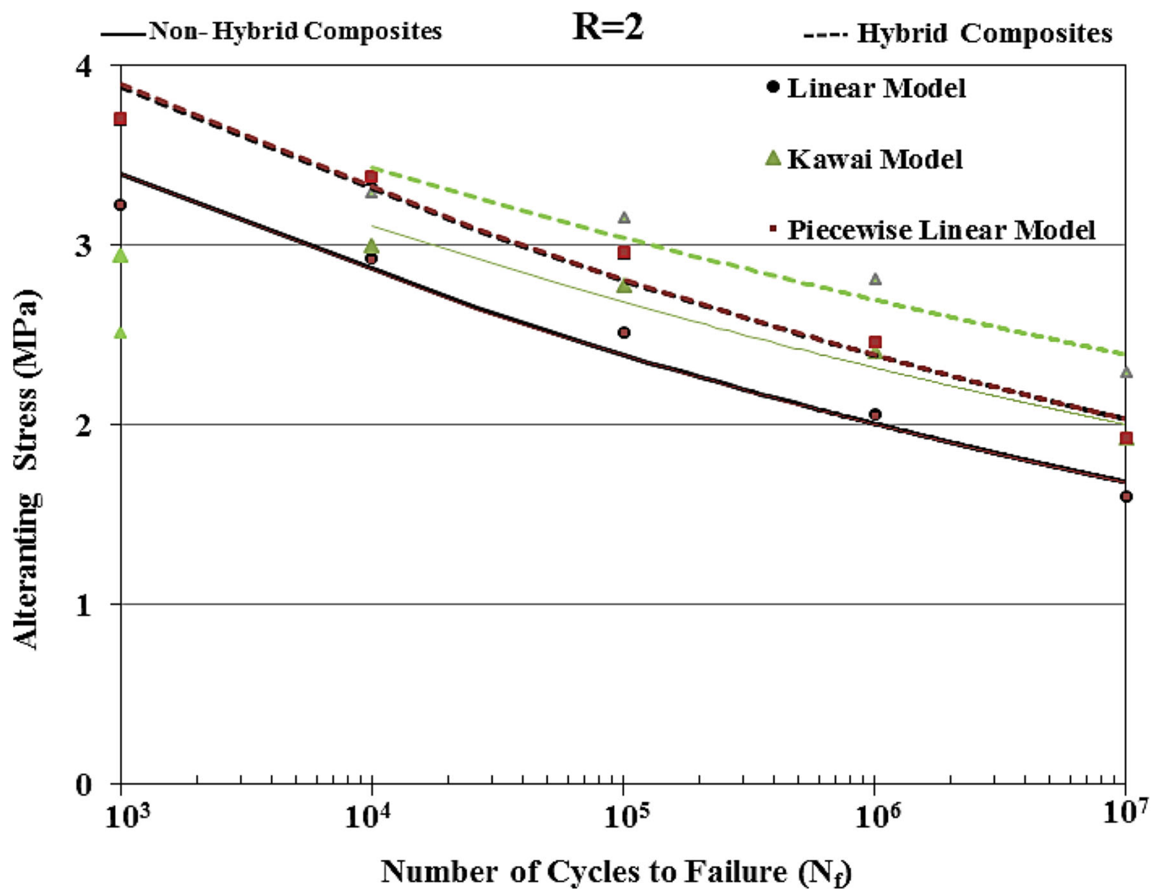

Fig. 10 *S–N* curves for $[NH]_4$ and $[H]_4$ composites at $R = 2$

under fatigue loads. Whereas Kawai's model exaggerates fatigue behavior of the $[NH]_4$ and $[H]_4$ composites, suggesting an overestimate of fatigue life and, as a result, it leads to non-conservative fatigue design. Hence, the piecewise linear model appears to be highly accurate and reliable CLD model for the full range of stress ratios investigated in this work. Therefore, designers may use a linear piecewise model to precisely draw constant life diagrams for accounting mean stress and anisotropy of materials on the fatigue strength of fiber-reinforced composites for varying stress ratios.

Conclusions

The effect of mean stress was studied for stress ratios, $R = 0.5$, 2, 0.1, − 0.5, − 2, and 10 using three constant life diagrams (CLDs) applied to composite materials. When compared to linear and Kawai's CLD models, the linear piecewise model is highly accurate for predicting the fatigue behavior of $[NH]_4$ and $[H]_4$ composites. By joining all the data points for the specified stress ratios, constant life curves were successfully drawn using linear piecewise model. The linear and Kawai's CLD models are less accurate for stress ratios $R = 0.5$ and 10. At these *R*-ratios,

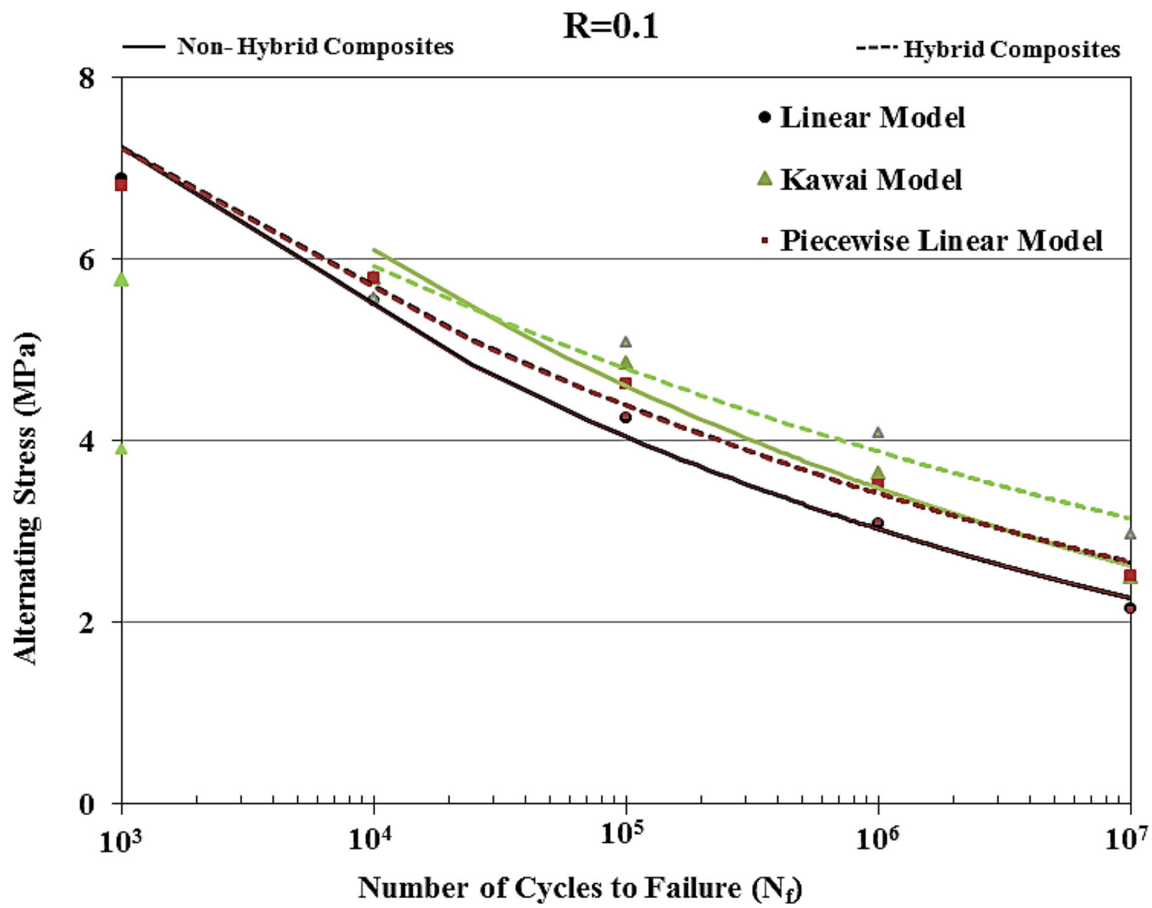

Fig. 11 *S–N* curves for $[NH]_4$ and $[H]_4$ composites at $R = 0.1$

constant life curves were unable to connect all data points. *S–N* predictions made by the linear model understate the fatigue strength of the $[NH]_4$ and $[H]_4$ composites for all stress ratios investigated, resulting in a conservative design under fatigue loads. In contrast, Kawai's model exaggerates fatigue behavior of the $[NH]_4$ and $[H]_4$ specimens, implying an overestimation of fatigue life and, as a result, it leads to non-conservative fatigue design. Therefore, for the entire range of R ratios investigated in this study, the piecewise linear model appears to be a highly accurate and reliable constant life diagram model.

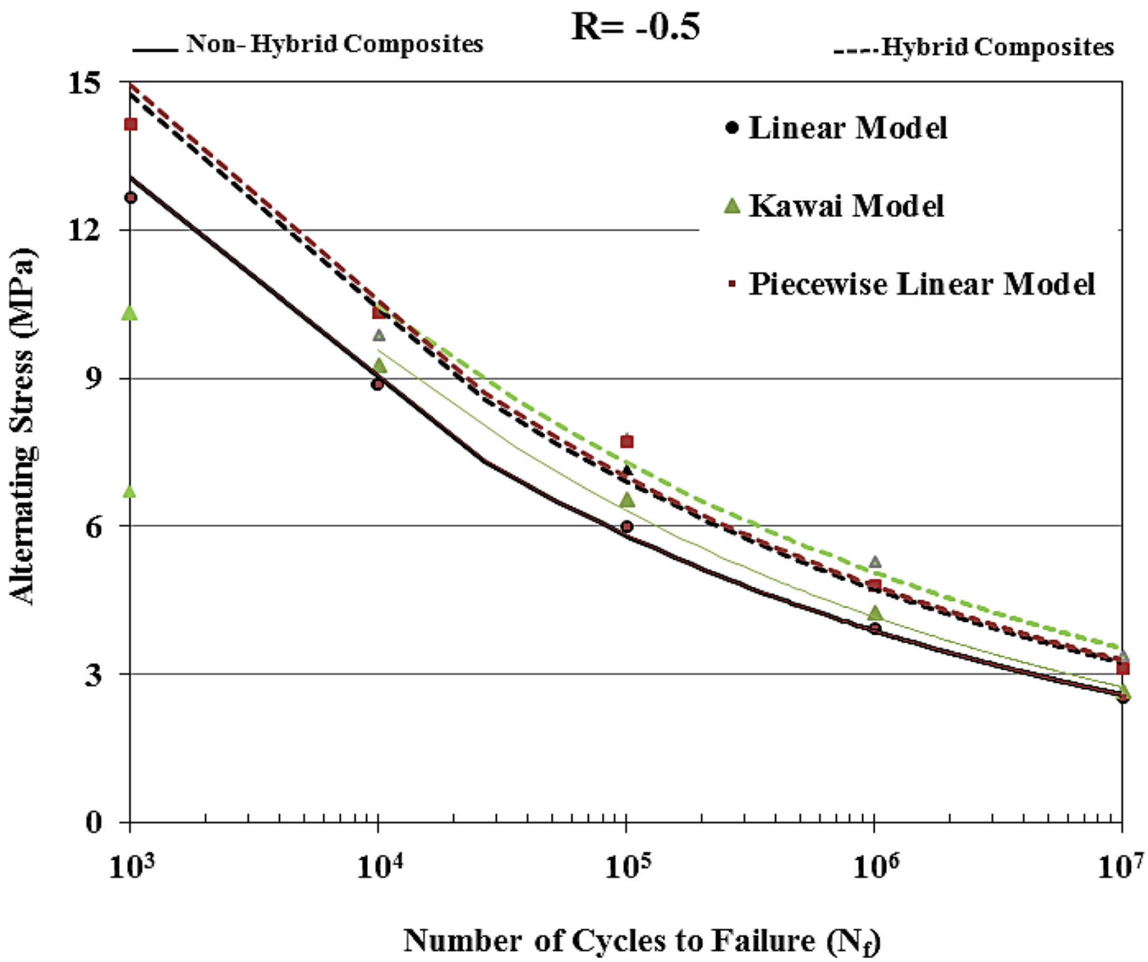

Fig. 12 *S–N* curves for $[NH]_4$ and $[H]_4$ composites at $R = -0.5$

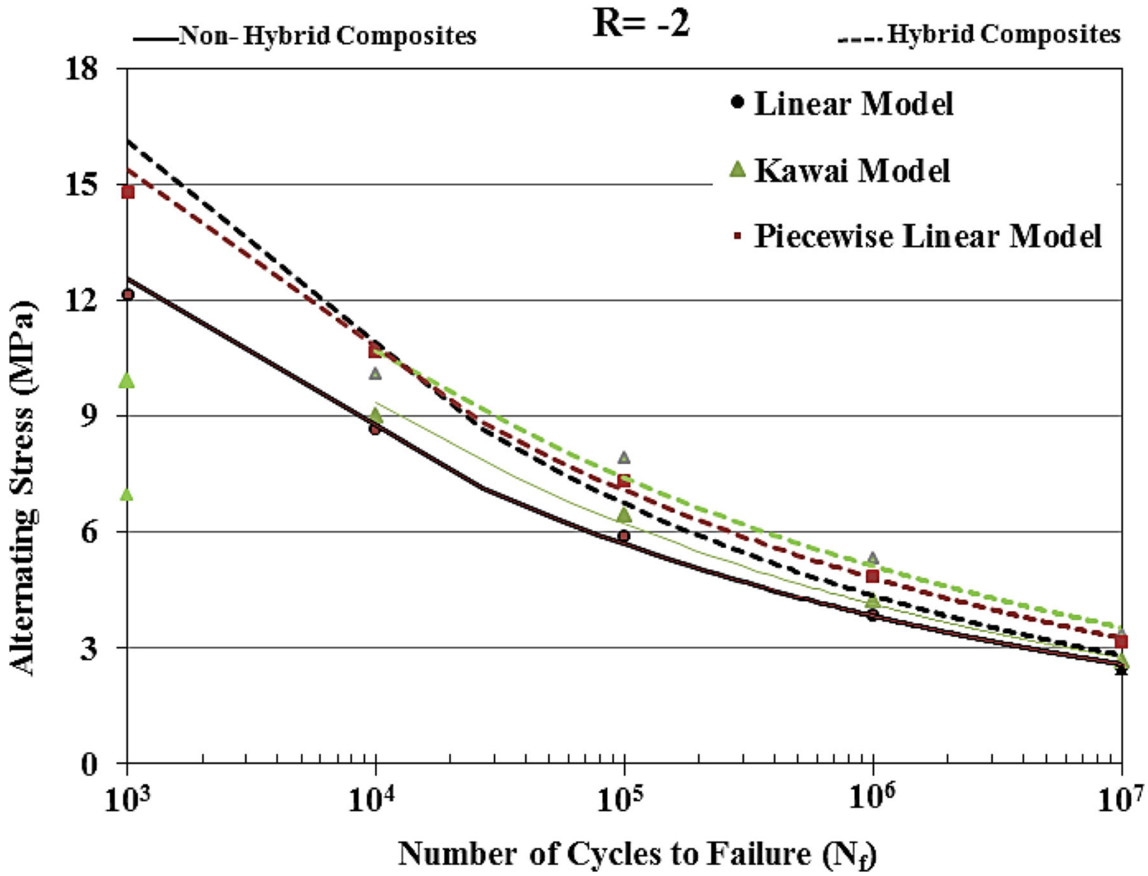

Fig. 13 *S–N* curves for $[NH]_4$ and $[H]_4$ composites at $R = -2$

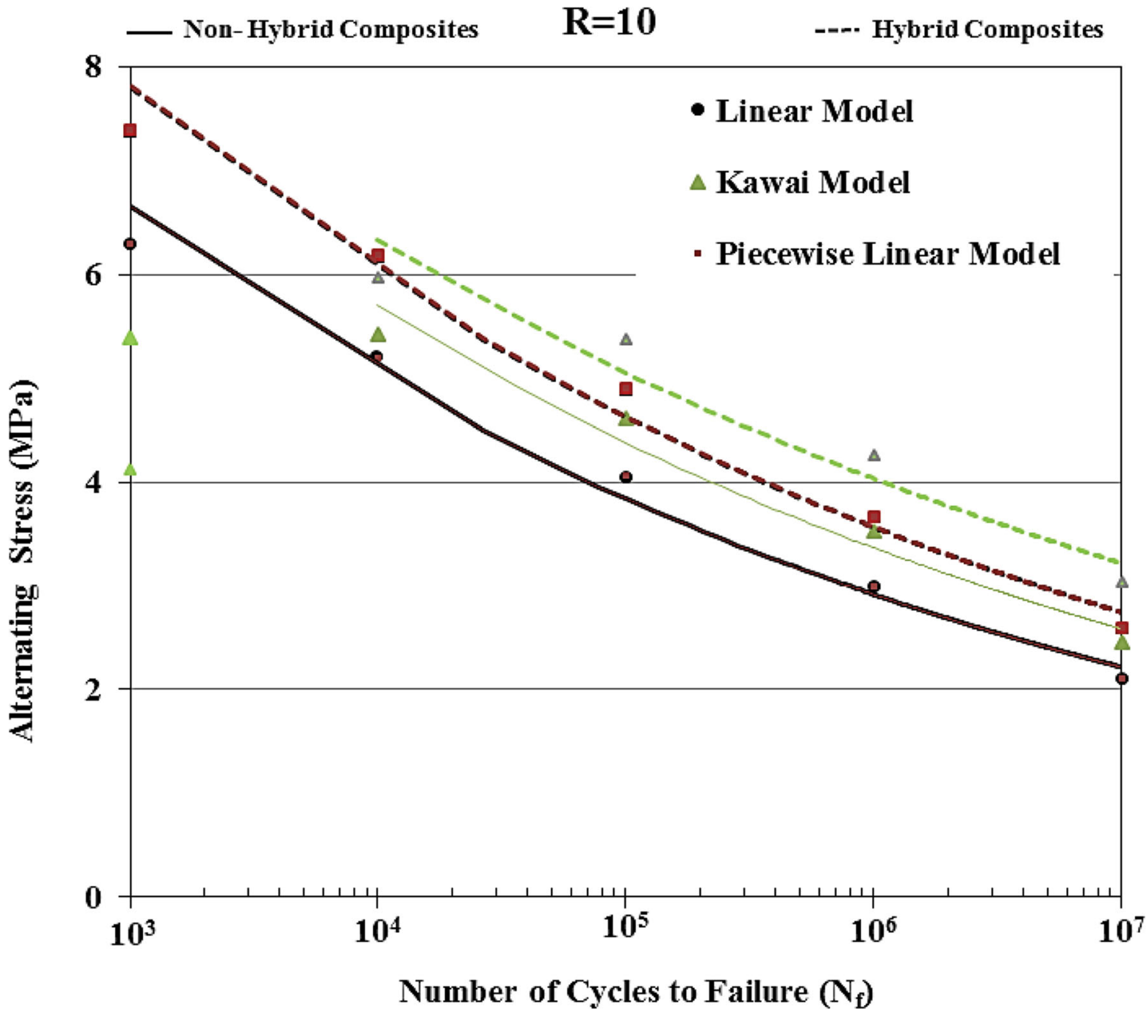

Fig. 14 *S–N* curves for $[NH]_4$ and $[H]_4$ composites at $R = 10$

Funding No funding organization in the private, public, or nonprofit sectors provided a specific grant for this research project.

Conflict of interest None declared.

Data Availability None.

References

1. C. Bathias, An engineering point of view about fatigue of polymer matrix composite materials. Int. J. Fatigue. **28**, 1094–1099 (2006)
2. M.M. Thawre, R.K. Paretkar, D.R. Peshwe et al., Construction of constant fatigue life diagram for a carbon fiber composite. Trans. Indian Inst. Met. **64**, 301–303 (2011)
3. T.P. Philippidis, A.P. Vassilopoulos, Complex stress state effect on fatigue life of GFRP laminates. Part I, experimental. Int. J. Fatigue. **24**(8), 813–23 (2002)
4. M.N.A. Nasr, M.N. Abouelwafa, A. Gomaa, A. Hamdy, E. Morsi, The effect of mean stress on the fatigue behavior of woven-roving glass fiber-reinforced polyester subjected to torsional moments. J. Eng. Mater. Technol. **127**(3), 301 (2005)
5. N.K. Kar, Y. Hu, E. Barjasteh, S.R. Nutt, Tension–tension fatigue of hybrid composite rods. Compos. Part B. **43**, 2115–2124 (2012)
6. P.K. Mallick, Y. Zhou, Effect of mean stress on the stress-controlled fatigue of a short E-glass fiber reinforced polyamide-6". Int. J. Fatigue. **26**, 941–946 (2004)
7. Y.H. Huh, J.H. Lee, D.J. Kim, Y.-S. Lee, Effect of stress ratio on fatigue life of GFRP composites for WT blade. J. Mech. Sci. Technol. **26**(7), 2117–2120 (2012)
8. S. Mortazavian, A. Fatemi. Effects of mean stress and stress concentration on fatigue behavior of short fiber reinforced polymer composites. Fatigue Fract. Engg. Mater. Struct. 001–18 (2015)
9. S. Liang, P.B. Gning, L. Guillaumat, A comparative study of fatigue behaviour of flax/epoxy and glass/epoxy composites. Compos. Sci. Technol. **72**(5), 535–543 (2012)
10. A.P. Vassilopoulos, B.D. Manshadi, T. Keller, Influence of the constant life diagram formulation on the fatigue life prediction of composite materials. Int. J. Fatigue. **32**, 659–669 (2010)

11. Amijima S, Tanimoto T, Matsuoka T. A study on the fatigue life estimation of FRP under random loading. Prog. Sci. Eng. Compos. 701–8 (1982)
12. T.P. Philippidis, A.P. Vassilopoulos, Life prediction methodology for GFRP laminates under spectrum loading. Compos. Part A. **35**(6), 657–66 (2004)
13. M. Kawai, M. Koizumi, Nonlinear constant fatigue life diagrams for carbon/ epoxy laminates at room temperature. Compos. Part A. **38**(11), 2342–53 (2007)
14. M. Kawai, A method for identifying asymmetric dissimilar constant fatigue life diagrams for CFRP laminates. Key Eng. Mater. **61–4**, 334–335 (2007)
15. C. Hemanth Kumar, R.P. Swamy, Experimental investigation on the fatigue behavior of glass fiber-reinforced epoxy composites under rotating bending loads. J. Fail. Anal. Prev. **21**, 582–587 (2021)